Preprints of the 21st IFAC World Congress (Virtual)
Berlin, Germany, July 12-17, 2020

Hybrid Automaton Control of Three Phase Reduced Switch Shunt Active Power Filter Connected Photovoltaic System

Z. Hekss*, A. Abouloifa*, J. M. Janik, I. Lachkar***, S. Echalih*, F. Z. Chaoui****, F. Giri****

** TI Lab, Faculty of Sciences Ben M'sick, Hassan II University of Casablanca, BP 7955 Casablanca, Morocco (Tel: +212 623 996 138; e-mail: zineb.hekss-etu@etu.univh2c.ma).*
***Normandie UNIV, UNICAEN, ENSICAEN, LAC, 14000 Caen, France*
****ESE Lab, ENSEM, Hassan II University of Casablanca, BP 8118 Casablanca, Morocco*
***** LMP2I Lab, ENSET, Mohammed V University, Rabat, Morocco*

Abstract: In this paper, a new controller design method based on hybrid automaton approach is proposed to solve the problem of controlling a three-phase reduced switch shunt active power filter (SAPF) connected to photovoltaic system. The control objective is two-fold: (i) ensuring a satisfactory power factor correction (PFC) by compensating the harmonic and reactive currents absorbed by the nonlinear load; (ii) regulating the voltage in the output of the photovoltaic panels to track a reference provided by the MPPT block in order to guarantee the power exchange between the photovoltaic source and three-phase electrical power grid. The considered control objectives are dealt with using a new two-loop cascaded controller. The hybrid automaton approach is applied in the inner loop, which ensures the operation modes of switching design in order to ensure a unity power factor. A proportional-integral (PI) regulator is used in the outer-loop to ensure the tight regulation of the voltage across the photovoltaic panels with a well-known P&O algorithm (MPPT). Finally, it is demonstrated through simulation results under Matlab/Simulink SimPowerSystems environment that the proposed automaton model and its controller can achieve the desired objectives.

Keywords: Shunt active power filter, PV system, Hybrid automaton model, MPPT, PI regulator, PFC.

1. INTRODUCTION

The increasing use of electronics loads into commercial and industrial applications have become major causes of the degradation of power quality due to its highly nonlinear structure. These nonlinear loads change the sinusoidal nature of the AC power current by drawing harmonic and reactive currents in the system which results in several effects including the distortion of the voltage waveform at the point of common coupling (PCC) and worsen power factor correction (PFC) performances (S. Echalih et al., 2019b).

Various studies proved the high dynamic performance of shunt active power filter (SAPF) to meet the harmonic standards. Many efforts have been made to develop the classical topologies for three-phase SAPF (Rahmani et al., 2010). In this way, the reduced switch SAPF, which presents reduced switch number converter less than a conventional full-bridge converter (Abouelmahjoub et al., 2018) has the advantages by using the minimum of semiconductors to offer increased speed and fewer control functions which results a higher filtering capability. The PV panels have received much attention with many feasible applications. SAPF connected photovoltaic systems are widely used as a better choice to transfer the real power to the nonlinear load and support reactive and harmonic power simultaneously, which can reduce the usage of electricity from the power grid (Z. Hekss et al., 2019b). A nonlinear control of single- phase SAPF connected PV systems based on sliding mode approach is addressed in (Z. Hekss et al., 2019a). The solar PV modules are characterized by a non-linear behavior that depending on environmental conditions such as solar irradiation and environment temperature which make difficult to predict the voltage and current to guarantee the maximum power production. According to the literature review, many various MPPT algorithms have been developed for PV power generation. P&O algorithm is presented in (Ishaque et al., 2014) as a reference method due to its efficacy and its ease of implementation. In most previous work, the most existing controllers are designed under the averaged nonlinear model for single-phase and three-phase SAPF whose principle is based on calculating average values of all the variables over one sampling period. A nonlinear control using Lyapunov technique is addressed to ensure PFC objective of reduced-part three-phase SAPF in (Abouelmahjoub et al., 2018). Recently, a hybrid automaton model is presented as a new switching design for power electronics systems (Senesky et al., 2003). The Hybrid automaton model allows the system to use powerful tools of the controller, which makes the possibility to take into account the continuous and discrete evolutions jointly. A new hybrid automaton control is introduced in (S. Echalih et al., 2019a), which the topology of SAPF based on interleaved buck converter.

In this paper, we propose a new approach of a control strategy that does not require an averaging model for three-phase reduced switch SAPF supplied by a photovoltaic generator and associated with nonlinear load. The control strategy consists of two loops: an inner loop of current control and an outer loop of voltage control. The controller inner-loop is designed using

the hybrid automaton in order to achieve a perfect power factor correction as possible. The outer loop is designed using a proportional-integral PI regulator to guarantee the MPPT issue with a well-known P&O algorithm for the regulation of DC-link capacitor voltage.

The paper is organized as follow: In section 2, the mathematical model and system description are described. Section 3 is devoted to the controller design of the system. The controller tracking performances are illustrated by numerical simulation showing the effectiveness of the proposed topology and controller in section 4. Finally, the paper ends with a conclusion in section 5.

2. SYSTEM DESCRIPTION AND MODELING

This section describes the modeling of three-phase reduced switch SAPF integrated with PV system as shown in Fig. 1. The system is composed of a three-phase supply voltage which include in series an internal impedance formed by a resistors and an inductors $(r_{gj}, L_{gj}\,; j = 1,2,3)$, nonlinear load and two photovoltaic panels connected to the three-phase power grid via a SAPF, which has a reduced switch number. A three-phase two-level IGBT based half-bridge inverters are employed to function as the SAPF with two identical capacitors values of energy storage C_{pv} placed on the DC side. In the AC side, the SAPF through a filtering impedance $\left(R_{fj}, L_{fj}\,; j = 1,2,3\right)$ is connected in parallel with a nonlinear load to the power grid. The nonlinear load consists of a full bridge rectifier with the resistive-inductive load.

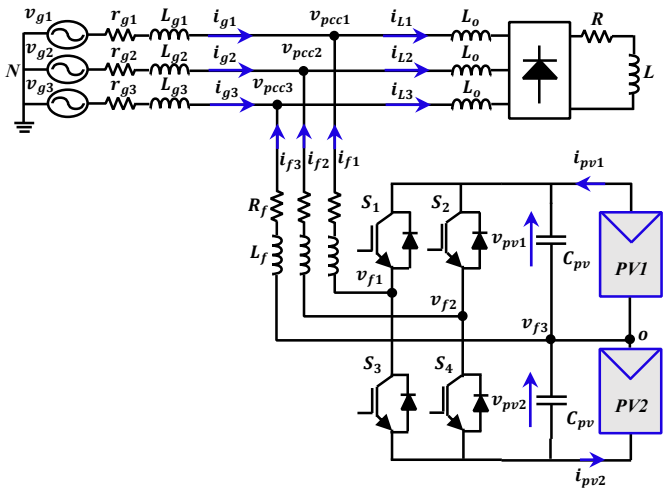

Fig. 1. Diagram of three phase reduced switch shunt active power filter connected to photovoltaic system.

The three-phase grid voltages $\left(v_{gj}(t)\,; j = 1,2,3\right)$ are supposed sinusoidal as follow:

$$v_{gj}(t) = E_g \sin\left(\omega_g t - \frac{2\pi}{3}(j-1)\right); j = 1,2,3 \qquad (1)$$

where E_g and ω_g denote respectively, the amplitude and the angular frequency of the three phase power grid. The resulting load currents $(i_{Lj}(t)\,; j = 1,2,3)$ are given by their Fourier expansion:

$$i_{Lj}(t) = \sum_{h=1}^{\infty} I_{L,h}\, sin(h(\omega_g t + \varphi_{j,h}))\;; j = 1,2,3 \qquad (2)$$

where $I_{L,h}$ and $\varphi_{j,h}$ denote, respectively, the amplitude and the phase of the harmonic current of order h.

2.1 Photovoltaic System:

In this work, we consider two identical photovoltaic array modules of 1STH-215-P type, built of N_p strings of photovoltaic modules connected in parallel. Each string consists of N_s modules connected in series. The corresponding electrical characteristics of 1STH-215-P module at nominal operating conditions *(G=1000 W/m², T = 25℃)* are listed in Table 1. The corresponding maximum power points (MPP) M1 to M3 are shown in Table 2.

Table 1. PV electrical parameters

Parameter	Symbol	Value
Maximum power	$\boldsymbol{P_m}$	213.15 W
Short circuit current	$\boldsymbol{I_{sc}}$	7.84 A
Open circuit voltage	$\boldsymbol{V_{oc}}$	36.3 V
Maximum power voltage	$\boldsymbol{V_m}$	29 V
Maximum power current	$\boldsymbol{I_m}$	7.35 A
Cells per module	$\boldsymbol{N_{cell}}$	60

Table 2. Maximum power points (MPP)

MPP	Irradiation Conditions (W/m^2)	Maximum voltage (V)	Maximum Power (W)
M1	1200	747.5	6253.84
M2	1000	754	5541.9
M3	800	758.94	4466.28

2.2 Instantaneous Model

This model takes into account the instantaneous states of the system. The switching functions μ_1 and μ_2 of the inverter taking values in the finite set {0, 1} as follows:

$$\mu_1 = \begin{cases} 1 \;if\; S_1\; is\; ON\; and\; S_3\; is\; OFF \\ 0 \;if\; S_1\; is\; OFF\; and\; S_3\; is\; ON \end{cases}$$

$$\mu_2 = \begin{cases} 1 \;if\; S_2\; is\; ON\; and\; S_4\; is\; OFF \\ 0 \;if\; S_2\; is\; OFF\; and\; S_4\; is\; ON \end{cases}$$

Applying Kirchhoff's laws, the instantaneous model of the three-phase reduced switch SAPF-PV is described by the differential equations as follows:

$$L_g \frac{d}{dt}\begin{pmatrix} i_{g1} \\ i_{g2} \\ i_{g3} \end{pmatrix} = -r_g \begin{pmatrix} i_{g1} \\ i_{g2} \\ i_{g3} \end{pmatrix} + \begin{pmatrix} v_{g1} \\ v_{g2} \\ v_{g3} \end{pmatrix} - \begin{pmatrix} v_{pcc1} \\ v_{pcc2} \\ v_{pcc3} \end{pmatrix} \qquad (3a)$$

$$L_f \frac{d}{dt}\begin{pmatrix} i_{f1} \\ i_{f2} \\ i_{f3} \end{pmatrix} = -R_f \begin{pmatrix} i_{f1} \\ i_{f2} \\ i_{f3} \end{pmatrix} + \begin{pmatrix} v_{f1} \\ v_{f2} \\ v_{f3} \end{pmatrix} - \begin{pmatrix} v_{pcc1} \\ v_{pcc2} \\ v_{pcc3} \end{pmatrix} \qquad (3b)$$

$$C_{pv} \frac{d}{dt}\begin{pmatrix} v_{pv1} \\ v_{pv2} \end{pmatrix} = \begin{pmatrix} i_1 \\ i_2 \end{pmatrix} \qquad (3c)$$

The power converter undergoes the following equations:

$$\begin{pmatrix} i_1 \\ i_2 \end{pmatrix} = \begin{pmatrix} i_{pv1} \\ i_{pv2} \end{pmatrix} + \begin{pmatrix} -\mu_1 & -\mu_2 \\ 1-\mu_1 & 1-\mu_2 \end{pmatrix} \begin{pmatrix} i_{f1} \\ i_{f2} \end{pmatrix} \qquad (4a)$$

$$\begin{pmatrix} v_{f1} \\ v_{f2} \\ v_{f3} \end{pmatrix} = \begin{pmatrix} v_{f1o} \\ v_{f2o} \\ 0 \end{pmatrix} + \begin{pmatrix} v_{on} \\ v_{on} \\ v_{on} \end{pmatrix} \quad (4b)$$

$$\begin{pmatrix} v_{f1o} \\ v_{f2o} \end{pmatrix} = \begin{pmatrix} \mu_1 & \mu_1 - 1 \\ \mu_2 & \mu_2 - 1 \end{pmatrix} \begin{pmatrix} v_{pv1} \\ v_{pv2} \end{pmatrix} \quad (4c)$$

Adding the three equations in (4b) and taking into account that the system of voltages (v_{f1}, v_{f2}, v_{f3}) is balanced, one gets:

$$v_{on} = -\frac{1}{3}\left((\mu_1 + \mu_2)v_{pv1} + (\mu_1 + \mu_2 - 2)v_{pv2}\right) \quad (4d)$$

Substituting (4d) in (4b) and using (4c) equations, one deduces that:

$$\begin{pmatrix} v_{f1} \\ v_{f2} \\ v_{f3} \end{pmatrix} = \frac{1}{3}\begin{pmatrix} 2\mu_1 - \mu_2 & 2\mu_1 - \mu_2 - 1 \\ -\mu_1 + 2\mu_2 & -\mu_1 + 2\mu_2 - 1 \\ -\mu_1 - \mu_2 & -\mu_1 - \mu_2 + 2 \end{pmatrix} \begin{pmatrix} v_{pv1} \\ v_{pv2} \end{pmatrix} \quad (4e)$$

This model is useful to build up the evolution at every moment of all the variables including the state of the switch (discrete location). However, the hybrid modeling is considered as one of the most suitable modeling methods to capture both continues and discrete dynamics of power converters, whose behavior is described by continuous nonlinear differential equations, and by an automat, with discrete-event dynamics behaviour (Benmansour et al., 2007) (Benmiloud et al., 2016).

2.3 Hybrid Model

The IGBT based inverter features four operation modes or four discrete states due to the switching action of (μ_1, μ_2) which are symbolled as $q_i (i = 1, 2, 3, 4)$. The state equations of each mode are described by affine continuous-time state-space equation as follow:

$$\dot{x} = f_{qi}(x) = A_{qi}x + B_{qi}\ ;\ i = 1, 2, 3, 4 \quad (5)$$

where the state of the system is defined as:

$$x = \left[i_{f1}, i_{f2}, v_{pv1}, v_{pv2}\right]^T \quad (6)$$

where (i_{f1}, i_{f2}) are the filter currents and (v_{pv1}, v_{pv2}) are the output voltages, which are equal to the capacitor voltages. Thus, the SAPF-PV system can be represented in terms of state equations correspond to a specific topology of converter for each mode, as follows:

Mode $(q = q_1)$, corresponds to $(\mu_1 = 0, \mu_2 = 0)$. The dynamic equations of the continuous variables are given by:

$$f_{q1}(x) = \begin{pmatrix} -\frac{R_f}{L_f} & 0 & 0 & -\frac{2}{3L_f} \\ 0 & -\frac{R_f}{L_f} & 0 & \frac{1}{3L_f} \\ 0 & 0 & 0 & 0 \\ 1 & 1 & 0 & 0 \end{pmatrix} x - \begin{pmatrix} \frac{v_{PCC1}}{L_f} \\ \frac{v_{PCC2}}{L_f} \\ i_{pv1} \\ i_{pv2} \end{pmatrix} \quad (7a)$$

Mode $(q = q_2)$, corresponds to $(\mu_1 = 0, \mu_2 = 1)$. The dynamic equations of the continuous variables are given by:

$$f_{q2}(x) = \begin{pmatrix} -\frac{R_f}{L_f} & 0 & -\frac{1}{3L_f} & -\frac{2}{3L_f} \\ 0 & -\frac{R_f}{L_f} & \frac{2}{3L_f} & \frac{1}{3L_f} \\ 0 & -1 & 0 & 0 \\ 1 & 0 & 0 & 0 \end{pmatrix} x - \begin{pmatrix} \frac{v_{PCC1}}{L_f} \\ \frac{v_{PCC2}}{L_f} \\ i_{pv1} \\ i_{pv2} \end{pmatrix} \quad (7b)$$

Mode $(q = q_3)$, corresponds to $(\mu_1 = 1, \mu_2 = 0)$. The dynamic equations of the continuous variables are given by:

$$f_{q3}(x) = \begin{pmatrix} -\frac{R_f}{L_f} & 0 & \frac{2}{3L_f} & \frac{1}{3L_f} \\ 0 & -\frac{R_f}{L_f} & -\frac{1}{3L_f} & -\frac{2}{3L_f} \\ -1 & 0 & 0 & 0 \\ 0 & 1 & 0 & 0 \end{pmatrix} x - \begin{pmatrix} \frac{v_{PCC1}}{L_f} \\ \frac{v_{PCC2}}{L_f} \\ i_{pv1} \\ i_{pv2} \end{pmatrix} \quad (7c)$$

Mode $(q = q_4)$, corresponds to $(\mu_1 = 1, \mu_2 = 1)$. The dynamic equations of the continuous variables are given by:

$$f_{q4}(x) = \begin{pmatrix} -\frac{R_f}{L_f} & 0 & \frac{1}{3L_f} & 0 \\ 0 & -\frac{R_f}{L_f} & \frac{1}{3L_f} & 0 \\ -1 & -1 & 0 & 0 \\ 0 & 0 & 0 & 0 \end{pmatrix} x - \begin{pmatrix} \frac{v_{PCC1}}{L_f} \\ \frac{v_{PCC2}}{L_f} \\ i_{pv1} \\ i_{pv2} \end{pmatrix} \quad (7d)$$

According to the following model, the hybrid automaton control of SAPF-PV system will be developed in the next section.

3. CONTROLLER DESIGN OF THE SYSTEM

In this section, we aim at designing a new controller design that will be able to ensure the two main objectives mentioned previously: (i) forcing the three phase grid currents to be a sinusoidal waveforms and in phase with the three phase grid voltages (PFC) by means of controlling SAPF-PV; (ii) regulating the DC-link voltage to track its reference provided by the MPPT block. The controller structure is based on two cascaded loops where its schematic diagram is shown in Fig.2.

3.1 Current Inner Loop Design

The power factor correction objective means that currents (i_{g1}, i_{g2}, i_{g3}) delivered by the three phase power grid must be sinusoidal signals and in phase with the grid voltages (v_{g1}, v_{g2}, v_{g3}) by tracking a reference signals $(i_{grefj} = \beta v_{gj}; j = 1, 2, 3)$. Indeed, the currents i_{f1} and i_{f2} injected by three-phase shunt active power filter should follow the best as possible the references i_{fref1}, i_{fref2} and $-(i_{fref1} + i_{fref2})$ respectively where:

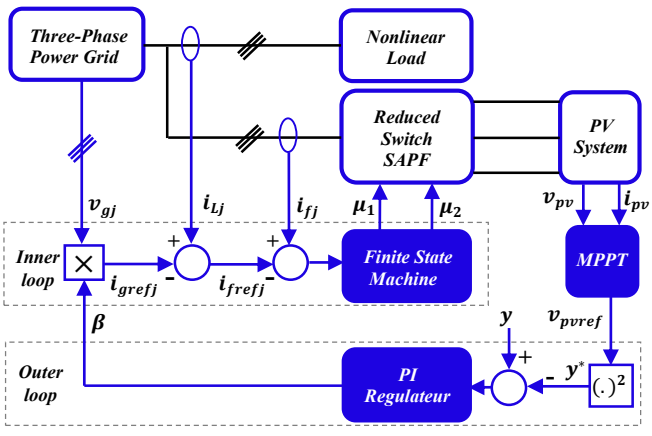

Fig. 2. Controller structure of reduced switch SAPF

$$\begin{pmatrix} i_{fref1} \\ i_{fref2} \end{pmatrix} = \begin{pmatrix} i_{L1} \\ i_{L2} \end{pmatrix} - \begin{pmatrix} i_{gref1} \\ i_{gref2} \end{pmatrix} \quad (8)$$

At this point, the parameter β is any real parameter that is allowed to be time-varying. The inner control loop will now be designed using the hybrid automaton, which is formulated below for the three-phase shunt active power filter. According to the paper (Benmansour et al., 2007), a hybrid automaton can be defined by the following system:

$$H = \{Q, X, F, I, E, G\} \quad (9)$$

where $Q = \{q_i, i\epsilon(1,2,3,4)\}$ is a finite set of four discrete states corresponding to system matrices for various operating modes (see equations 7a-d); $X = \Re^4$ is the continuous state space that characterizes the operating modes of the converter; $F: Q \times X \longrightarrow \Re^4$ is the vector field associated with each discrete state; $I \subset Q \times X$ is a set of possible initial conditions; $E \subset Q \times Q$ is the set of the possible transitions in the automaton; $G: E \longrightarrow 2^X$ is the constraint in the continuous field for validating a transition $e\epsilon E$; is also called the guard condition. In this case, the hybrid automaton can operate in four distinct modes; the switching between these modes is governed by finite state machine (FSM). Based on the currents injected by three-phase shunt active power filter and its references, we can thus give the conditions of selecting each mode:

$$Mode1\ (q_1) = \{x \in \Re^4 / \ i_{f1} < i_{fref1} \wedge i_{f2} < i_{fref2}\} \quad (10a)$$

$$Mode2\ (q_2) = \{x \in \Re^4 / \ i_{f1} < i_{fref1} \wedge i_{f2} > i_{fref2}\} \quad (10b)$$

$$Mode3\ (q_3) = \{x \in \Re^4 / \ i_{f1} > i_{fref1} \wedge i_{f2} < i_{fref2}\} \quad (10c)$$

$$Mode4\ (q_4) = \{x \in \Re^4 / \ i_{f1} > i_{fref1} \wedge i_{f2} > i_{fref2}\} \quad (10d)$$

The set of possible transitions (guard conditions) $G(T_{ij}) = G(q_i, q_j)$ between various modes are defined by the following equations:

$$G(T_{21}) = G(T_{31}) = G(T_{41}) = \{i_{f1} < i_{fref1} \wedge i_{f2} < i_{fref2}\} \quad (11a)$$

$$G(T_{12}) = G(T_{32}) = G(T_{42}) = \{ i_{f1} < i_{fref1} \wedge i_{f2} > i_{fref2}\} \quad (11b)$$

$$G(T_{13}) = G(T_{23}) = G(T_{43}) = \{ i_{f1} > i_{fref1} \wedge i_{f2} < i_{fref2}\} \quad (11c)$$

$$G(T_{14}) = G(T_{24}) = G(T_{34}) = \{ i_{f1} > i_{fref1} \wedge i_{f2} > i_{fref2}\} \quad (11d)$$

The diagram of the controller as shown in Fig. 3 presents the three-phase reduced switch SAPF-PV in the form of a hybrid automaton (state finite machine).

3.2 Voltage outer loop design

The objective of this part is the regulation of the voltage in the output of photovoltaic system to track a reference signal provided by the MPPT block in order to guarantee the power exchange between the source and AC grid.

3.2.1 PV generator reference voltage

In this work, the MPPT algorithm is applied to the reference of the outer loop control DC using the P&O algorithm due to its simplicity of implementation and a fewer measured parameter, where it needs two input signals which are i_{pv} and v_{pv} to provide the voltage v_{pvref} which the photovoltaic

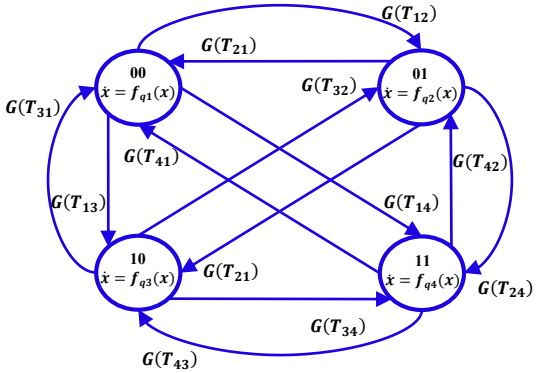

Fig. 3. Hybrid automaton

voltage must track. The algorithm steps are described as shown in flowchart in the paper (Ishaque et al., 2014).

3.2.2 DC bus voltage regulation

Now, we aim to generate a tuning law for the ratio β in such a way that the output photovoltaic voltage ($v_{pv} = v_{pv1} + v_{pv2}$) will be regulated to a given reference signal ($v_{pvref} = v_{pv1ref} + v_{pv2ref}$) using a PI controller.

- Relation between β and v_{pv}:

The first step in designing such a loop is to establish a relationship between β (the control signal) and the output voltage v_{pv}. This is the subject of the following proposition.

Proposition 1: Considering the three-phase reduced switch SAPF integrated with photovoltaic system described by its hybrid model (7a-d) and using the energy conservative law $(P_L = P_g + P)$ under the following assumptions:

- The current inner loop is faster than the voltage outer loop (i.e. $i_{gj} = \beta v_{gj}; j = 1,2,3$).
- $(r_{gj}, L_{gj}, R_{fj}, L_{fj}; j = 1,2,3)$ are negligible.
- The two PV panels have the same characteristics.

Then, we have the following results:

The output voltage v_{pv} varies in response to the signal β by the following equation:

$$C_{pv}\frac{dv_{pv}}{dt} = \frac{1}{v_{pv}}\left(3\beta {E_g}^2 - \frac{3}{2}E_g I_{L1}\cos\varphi_1\right) \quad (14)$$

I_{L1}: Load instantaneous fundamental phase current.
φ_1: Phase difference between grid voltage and grid current.

1) The squared-voltage $y = {v_{pv}}^2$ is described by the following first order time-varying linear equation:

$$\frac{dy}{dt} = \frac{1}{C_{pv}}\left(3\beta {E_g}^2 - \frac{3}{2}E_g I_{L1}\cos\varphi_1\right) \quad (15)$$

- Squared output voltage regulation:

The signal β stands as a control input in the first-order system (15). The problem is to design a suitable control law so that the squared voltage $y = {v_{pv}}^2$ tracks a given reference signal $y^* = {v_{pvref}}^2$. To this end, a PI regulator is considered:

$$\beta = \left(k_p + \frac{k_i}{s}\right)(y - y^*) \quad (16)$$

where the regulator parameters (K_p, K_i) are any positive real constants. In closed-loop system, the dynamic behaviour control of y is given by the following equation:

$$y = G(s)P_L - F(s)y^* \quad (17)$$

with

$$G(s) = \frac{2sP_L}{C_{pv}s^2 + 6E_g^2 k_p s + 6E_g^2 k_i}$$

$$F(s) = \frac{6E_g^2 k_p s + 6E_g^2 k_i}{C_{pv}s^2 + 6E_g^2 k_p s + 6E_g^2 k_i}$$

Furthermore, if $\varepsilon \to 0$, the squared voltage y converge to its reference value y^*. Specifically, one has:

$$\lim_{s\to 0} y = \lim_{t\to\infty} y = y^* \quad (18)$$

Then, the DC bus voltage regulation is actually achieved.

4. SIMULATION RESULTS

In this section, the performance of the proposed reduced switch SAPF connected to the photovoltaic system utilizing the new controller method based on a hybrid automaton model is numerically evaluated in Matlab/Simulink with the proposed parameters as shown in Table 3. The simulation work is conducted under balanced and distorted conditions, which involve a nonlinear load at standard climatic conditions (G=1000 W/m^2 and T=25℃) and with changes in solar irradiation conditions. The total harmonic distortion (THD) of grid current mitigated by SAPF-PV system are also measured to evaluate the performance of the proposed controller, which its values are summarized in Table 4.

Table 3. The parameters of the system and the controller

Parameter	Symbol	Value
Three phase power grid	v_g	230 V/ 50 Hz
	r_g	2 mΩ
	L_g	0.2 mH
Nonlinear load	L	500 mH
	R	15 Ω
	L_o	5 mH
Photovoltaic system	N_p	1
	N_s	26
Reduced switch SAPF	R_f	8 mΩ
	L_f	3 mH
	C_{pv}	6 mF
Voltage regulator	K_p	$4x10^{-3}$
	K_i	$1x10^{-4}$

4.1 Control performance at standard climatic conditions

The simulation results obtained at standard climatic conditions are shown in Figs 4-8. Fig. 4 show the three-phase load current waveforms, which are clearly presents a harmonic distortion due to nonlinear load, which create harmonic currents in a three-phase power system. Figs. 5-8 show the excellent robustness of the proposed controller. The available real power extracted from the photovoltaic generator is transferred to the power system, which shows that the regulation of the voltage across the photovoltaic panels tracks its maximum reference provided by the MPPT block as shown in Fig. 5. Fig. 6 shows that the filter current injected in the power grid converges to its reference value with a good accuracy. Fig. 7 clearly indicates that the grid current has sinusoidal waveform with a lower THD value and kept in phase with grid voltage. Then Fig. 8 shows that the evolution of control signal β takes constant value after the transient period, which kept the unitary power factor.

4.2 Control performance with changes in solar irradiation

The performances of the designed controller in the above section are checked considering the changing of irradiation conditions with the obtained results as presented in Figs 9-10. Firstly, the irradiance G has decreased from 1 kW/m^2 to 0,8 kW/m^2 at *0.7s* while the temperature is kept constant T= *25℃*. It is seen that the controller keeps the whole system at the optimal operation conditions. The real power extracted from each photovoltaic panels is decreased between 5541,9 W and 4466,28 W corresponding to the maximum points M2 and M3 of (Table 2), where the amplitude of the grid current is increased and kept in phase with the grid voltage as shown in Fig. 9. Secondly, the irradiation is changed from 0,8 kW/m^2 to 1,2 kW/m^2 at *1.3s* while the temperature is kept constant. The photovoltaic power from each panels is increased between 4466,28 W and 6253,84 W corresponding to M3 and M1 (see Table 2), where the grid current is decreased and also proves the PFC achievement as shown in Fig.10, which shows that the maximum power provided by the photovoltaic panels is totally injected into the electrical power grid. This is further demonstrated by Fig. 11, that the control signal β always takes a constant value each time the power factor correction is ensured.

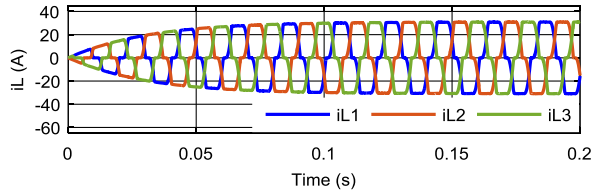

Fig. 4. Three phase load current waveforms

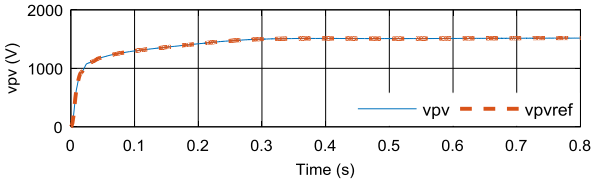

Fig. 5. PV voltage waveform and its reference

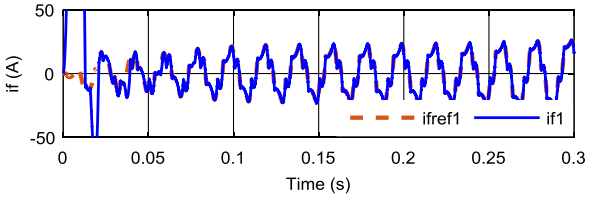

Fig. 6. Filter current waveform and its reference

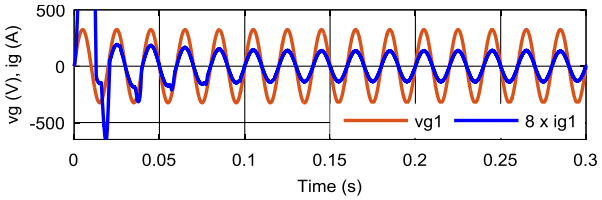

Fig. 7. Check of the power factor

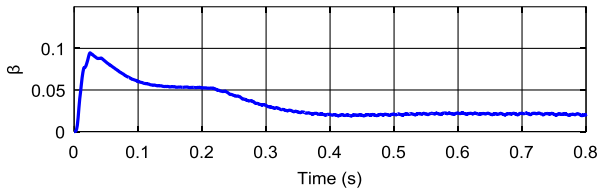

Fig. 8. External control signal β waveform

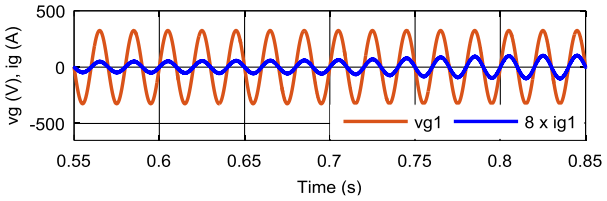

Fig. 9. Unity PFC under irradiation changes

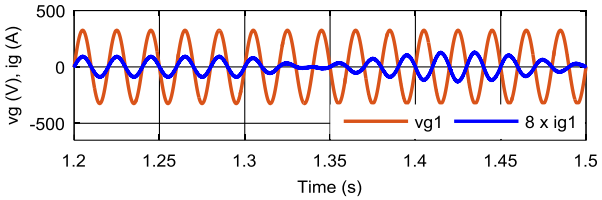

Fig. 10. Unity PFC under irradiation changes

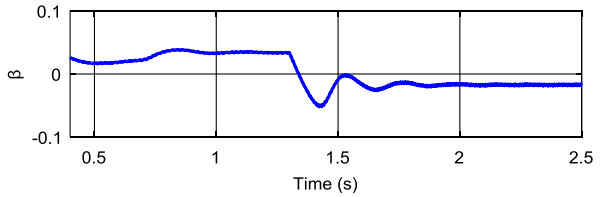

Fig. 11. External control signal β under irradiation changes

Table 4. THD Results of Mitigated Grid Current

Climatic conditions	Total Harmonic Distortion, THD (%)
	Before connecting SAPF-PV
	27.73%
	After connecting SAPF-PV
G=1000W/m²; T=25℃	1.38%
G=800W/m²; T=25℃	2.40%
G=1200W/m²; T=25℃	3.07%

5. CONCLUSIONS

In this paper, a new controller design method has been developed using the hybrid automaton approach for three-phase SAPF supplied by photovoltaic system and associated with nonlinear load. The simulation results obtained in this work show that the proposed controller provides better performance under different operating conditions for which it was designed. The hybrid automaton model is successfully controlling the system to achieve lower THD values, which complies with the international IEEE standard. The regulation of the voltage across the photovoltaic panels provides perfect MPPT with P&O algorithm. Finally, it is formally established that the control objectives are actually achieved, including PFC requirement, extracting a maximum power from the PV array and DC-link voltage regulation.

REFERENCES

Abouelmahjoub, Y., Giri, F., Abouloifa, A., Chaoui, F. Z., and Kissaoui, M. (2018). Adaptive Nonlinear Control of Reduced-Part three-Phase Shunt Active Power Filters. *Asian Journal of Control*, 20, 1720–1733.

Benmansour, K., Benalia, A., Djemaï, M., and De Leon, J. (2007). Hybrid control of a multicellular converter. *Nonlinear Analysis: Hybrid Systems* 1, 16–29.

Benmiloud, M., Benalia, A., Defoort, M., and Djemai, M. (2016). On the limit cycle stabilization of a DC/DC three-cell converter. *Control Engineering Practice*, 49, 29–41.

Echalih, S., Abouloifa, A., Hekss, Z., and Lachkar, I. (2019). Half Wave Control Strategy of Interleaved Buck Converter Based Single Phase Active Power Filter for Power Quality Improvement, *In 2019 4th World Conference on Complex Systems (WCCS)* (pp.1–6). Ouarzazate, Morocco. IEEE.

Echalih, S., Abouloifa, A., Lachkar, I., Hekss, Z., Aourir, M., and Giri, F. (2019). Hybrid Control of Single Phase Shunt Active Power Filter Based on Interleaved Buck Converter, *In 2019 American Control Conference (ACC)* (pp. 3636–3641). Philadelphia, PA, USA. IEEE.

Hekss, Z., Abouloifa, A., Echalih, S., and Lachkar, I. (2019). Cascade Nonlinear Control of Photovoltaic System Connected to Single Phase Half Bridge Shunt Active Power Filter, *In 2019 4th World Conference on Complex Systems (WCCS)* (pp. 1–6). Ouarzazate, Morocco. IEEE.

Hekss, Z., Lachkar, I., Abouloifa, A., Echalih, S., Aourir, M., and Giri, F. (2019). Nonlinear Control Strategy of Single Phase Half Bridge Shunt Active Power Filter Interfacing Renewable Energy Source and Grid, *In 2019 American Control Conference (ACC) (pp. 1972–1977)*. Philadelphia, PA, USA. IEEE.

Ishaque, K., Salam, Z., and Lauss, G. (2014). The performance of perturb and observe and incremental conductance maximum power point tracking method under dynamic weather conditions. *Applied Energy*, 119, 228–236.

Rahmani, S., Mendalek, N., and Al-Haddad, K. (2010). Experimental Design of a Nonlinear Control Technique for Three-Phase Shunt Active Power Filter. *IEEE Transactions on Industrial Electronics*, 57(10), 3364-3375.

Senesky, M., Eirea, G., and Koo, T. J. (2003). Hybrid Modelling and Control of Power Electronics. *In International Workshop on Hybrid Systems: Computation and Control* (pp. 450-465). Springer, Berlin, Heidelberg.